



ANALYTICAL STUDY ON SEISMIC PERFORMANCE OF A CONTINUOUS RIGID FRAME BRIDGE WITH UNEQUAL PIERS CONSIDERING DAMAGE GROWTH AND ENERGY ABSORPTION

Tomohisa HAMAMOTO¹, Taiji MAZDA², Hisanori OTSUKA³, And Nayoko HAMADA⁴

SUMMARY

In this paper, it was specified that the check of seismic performance took the plasticity parts of concrete pier into consideration by Specifications for Highway Bridges Part V ; Seismic Design¹⁾ (Specification V is called hereafter) revised in 2002. Generally speaking, the plastic modification of a concrete pier may occur in two or more places in case of the in-plane direction's earthquake on a continuous rigid frame bridge. Moreover, it can be plentifully seen that the case where a static seismic judgment result of safety produces a big difference to a dynamic response analysis result. On the other hand, it is important on a design to perform the examination by reference of seismic performance, after being exactly based on an ultimate limit state of the whole bridge. By this study, its attention was paid to the damage growth and the energy absorption in each plastic hinge part of the continuation rigid frame bridge from such a viewpoint. Here, pushover analysis and dynamic response analysis were carried out for the longitudinal direction to the bridge axis.

INTRODUCTION

Generally, a continuous rigid frame bridge is a bridge where the action in case of an earthquake is complicated. In Japanese business design, seismic performance is checked in many cases by dynamic response analysis after carrying out static examination by reference. Moreover, the static seismic design method (Verification of the seismic performance based on the ductility method) is considered to be the design technique by the side of safety to the seismic motion caused by a magnitude 7 class inland direct strike type earthquake that occurs very infrequently such as the 1995 Hyogo-ken Nanbu Earthquake (level2 earthquake motion is called hereafter), and to the seismic motion of short duration but high intensity. Next, it is required to evaluate appropriately damage progress process until a continuous rigid frame bridge approaches an ultimate limit state, and to attain rationalization of a seismic design. In order to deepen such an argument, writers²⁾ were checking the following things to a continuous rigid frame bridge with unequal pier height, and with columns that the ultimate horizontal strength differed.

¹ Tomohisa HAMAMOTO, Pacific Consultants Co.,Ltd., Japan, E-mail:tomohisa.hamamoto@os.pacific.co.jp

² Taiji MAZDA, Kyusyu University, Fukuoka, Japan, E-mail: mazda@doc.kyushu-u.ac.jp

³ Hisanori OTSUKA, Kyusyu University, Fukuoka, Japan, E-mail: otsuka@doc.kyushu-u.ac.jp

⁴ Nayoko HAMADA, Kyusyu University, Fukuoka, Japan, E-mail: hamada@doc.kyushu-u.ac.jp

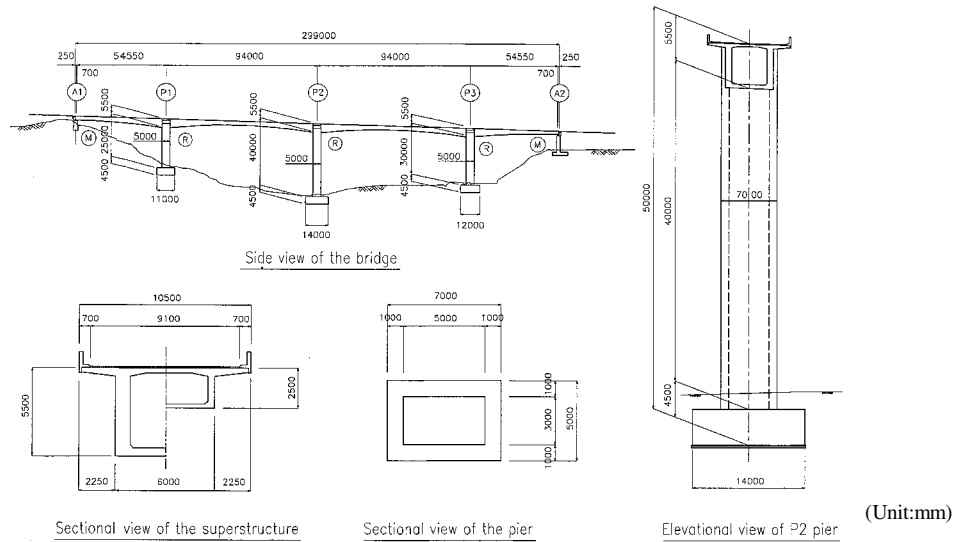


Fig.1 Outline of the bridge for analysis

In the progress process of bending damage, it was checking that the influence of unequal pier height affected the maximum response ductility factor, after all plastic hinge parts reached the yield limit state.

By this study, its attention was paid to the damage growth and the energy absorption in each plastic hinge part of the continuation rigid frame bridge from such a viewpoint. Here, pushover analysis and dynamic response analysis were carried out to the longitudinal direction to the bridge axis for a continuous rigid frame bridge with unequal piers. Furthermore, these were also carried out about transition of the maximum response ductility factor in the plastic hinge part, and about attention to the damage index of the plastic hinge part.

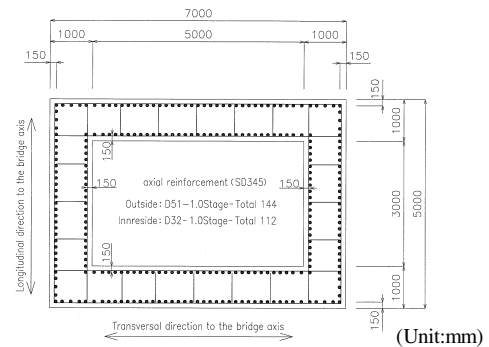


Fig.2 Detail of reinforcement

ANALYTICAL CONDITION

This examination was aimed at the continuous rigid frame bridge crossed over a length of 299m (refer to Fig.1). For span of 54.55+94.00+94.00+54.55m, this bridge had the structure preface with unequal pier height that P1 bridge pier height was 25m, P2 bridge pier height was 40m, P3 bridge pier height was 30m. The material characteristic of the superstructure was used as the nonlinear beam element. The material characteristic of a bridge pier part was used as the nonlinear beam element that has surrender rigidity. It was based on the bridge pier section shown in Fig.2. However, the plastic hinge parts were set to the vertical end of a bridge pier. The nonlinear rotation spring constant was prepared in the center of a plastic hinge domain. The analysis model is shown in Fig.3. As shown in Fig.3, the linear spring constant of vertical, horizontal, and rotation considering the dynamic modification coefficient of the ground was prepared in the lower end of the footing of a bridge pier. Since its attention was paid to the modification performance of only a bridge pier in case static analysis was performed, the bottom end of a bridge pier was considered as fixation. The foundation type of a bridge was the spread foundation, and it set up with a bridge built on Ground Type I. The modification factor for regional Class A was used as 1.0 for regions A, and the classification of importance was used Bridges of Class B. Moreover, the bending failure type of the whole bridge system set up the analysis model that the bending failure of a bridge pier will occur first, and that superstructure was not made to surrender. In dynamic response analysis, the

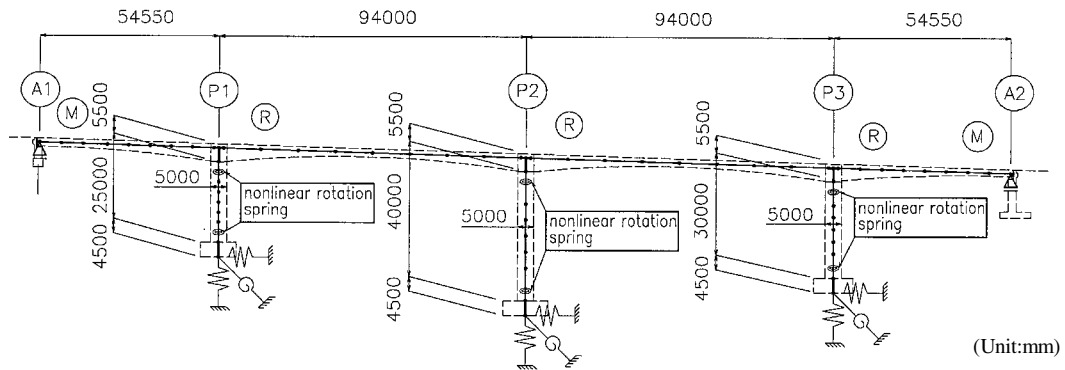


Fig.3 Analysis model

integration time interval was made into 0.001 seconds using the New Mark β method ($\beta = 0.25$). Furthermore, three wave forms (TYPE II - I - 1, TYPE II - II - 1, TYPE II - III - 1) of the acceleration wave form which adjusted the amplitude of a typical past strong motion record on the frequency zone by making Specification V reference as level 2 earthquake motion were used for the input earthquake motion. The cycle of the sinusoidal wave on this bridge was made into the cycle in the primary mode that the effective mass ratio obtained from eigenvalue analysis stood high. The wave forms of the input earthquake motion used for this examination are shown in Fig. 4 (a) ~ (d). The damping factors of each part material used when calculating the mode damping constant by energy proportionality type attenuation were superstructure : 3%, general part of the concrete pier : 5%, plastic hinge part of the concrete pier : 2%, and foundation structure : 20%. General-purpose structural analysis program TDAPIII was used for analysis software.

ANALYSIS RESULTS

1. Bending damage growth in static analysis results

In this chapter, the technique of static analysis was used pushover analysis. Here, in order to evaluate progress of the bending damage by unequal pier height clearly, the vibration direction examined two

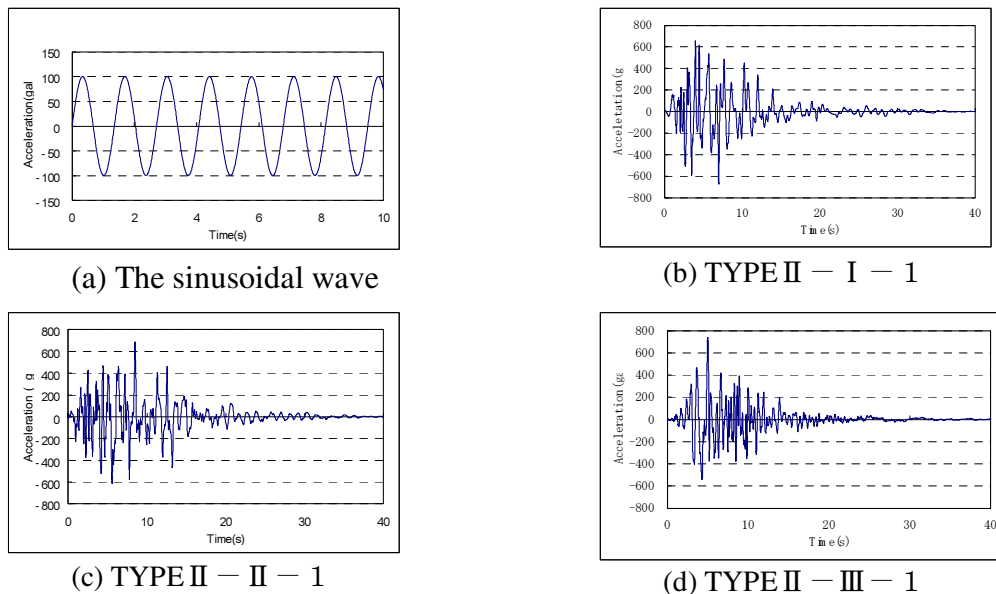
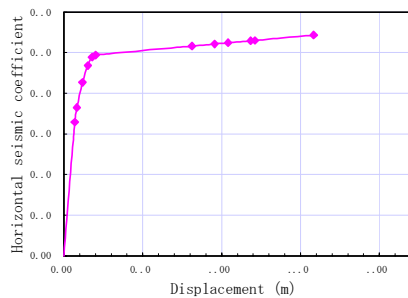


Fig.4 Input earthquake waves

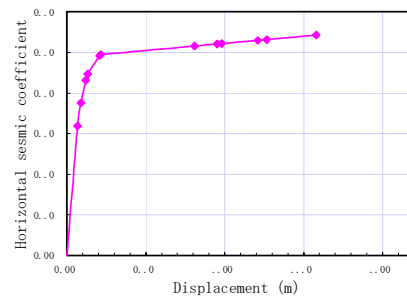
directions. Pushover analysis using the static analysis technique was made to act progressively as horizontal load on each bridge pier and superstructure. The vibration direction considers the case where horizontal load is made to increase gradually in the direction of $P1 \rightarrow P3$, and the direction of $P1 \leftarrow P3$ from having unequal bridge pier height. The yield order, superstructure displacement, and design seismic coefficients surrendered are collectively shown in Fig.5. In the input time of the direction of $P1 \rightarrow P3$, the bottom end of P1 bridge pier reached the yield limit state first, next the bottom end of P3 bridge pier reached the yield limit state, and finally the bottom end of P2 bridge pier reached the yield limit state. Then, the yield limit state is reached in order of P3 bridge pier top end, P1 bridge pier top end, and P2 bridge pier top end. In the input time of the direction of $P1 \leftarrow P3$, the bottom end of P1 bridge pier reached the yield limit state first, next the bottom end of P3 bridge pier reached the yield limit state, and finally the bottom end of P2 bridge pier reached the yield limit state. Then, the upper end of P1 bridge pier top end results in a yield limit state first. Subsequently, the yield limit state is reached in order of P2 bridge pier top end and P3 bridge pier top end. Furthermore, as compared with the bottom end of P2 bridge pier having reached the limit state in the input time of the direction of $P1 \leftarrow P3$, the limit state is reversed in the input time of the direction of $P1 \leftarrow P3$ about bending damage growth of the ultimate limit state. Therefore, the order of bending damage growth differs by the input time of the direction of $P1 \rightarrow P3$ and the input time of the direction of $P1 \leftarrow P3$. The reason the order of damage progress differs is considered that the change of bridge pier height has influenced. In this pushover analysis results, it has checked that the order of bending damage growth changed with the vibration direction.

2. Results of eigenvalue analysis

In this section, the continuous rigid frame bridge for analysis will be a bridge where the action in case of an earthquake is complicated. Then, it will be required to grasp the oscillation characteristic. Therefore, eigenvalue analysis was carried out in order to check an oscillation characteristic. The Rayleigh damping



(a) In the input time of the direction of $P1 \rightarrow P3$



(b) In the input time of the direction of $P1 \leftarrow P3$

Fig.5 Results of static analysis

Table 1 Results of eigenvalue analysis

Degree	Natural frequency (Hz)	Fundamental natural period (s)	Effective mass ratio	Damping ratio
1	0.752390	1.32910	67.0%	0.082700
2	1.406300	0.71107	67.0%	0.039355
3	1.909500	0.52371	67.0%	0.037190
4	2.882600	0.34691	74.0%	0.041160
5	3.196300	0.31286	75.0%	0.041031
6	3.954300	0.25289	77.0%	0.055000
7	4.543400	0.22010	77.0%	0.049615
8	4.786600	0.20892	77.0%	0.067095
9	4.950800	0.20199	79.0%	0.127218
10	6.006800	0.16648	90.0%	0.148372

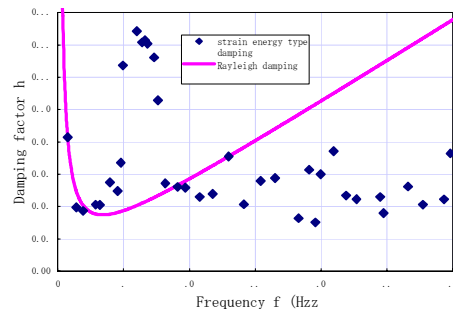


Fig.6 Modal damping

[C] specified by the following formulas based on the result which carried out eigenvalue analysis estimated the damping constant used in dynamic response analysis.

$$[C] = a [M] + b [K]$$

Here, [C] : Damping matrix
[M] : Mass matrix
[K] : Stiffness matrix
a, b : Coefficient

Here, coefficients of a and b defined the damping constant h to the bridge pier and the foundation structure part, respectively, and set it up from the mode damping constant calculated based on an analysis result. Moreover, the primary mode in which an effective mass ratio stands high, and the damping effective mass ratio chose and set up the 18th mode used as 100%. Modal damping is shown in Fig.6. Furthermore, the analysis result to the 10th mode is shown in Table 1. In this analysis model, the effective mass ratio in the primary mode has become about 67% of the whole system. Therefore, generally it is thought that a bridge like a continuous rigid frame bridge cannot disregard influence of oscillating mode in longitudinal direction to the bridge axis.

3. Bending damage growth in dynamic response analysis results

In this dynamic response analysis, three wave forms of the input earthquake motion that the frequency characteristic differed and the sinusoidal wave was resonating on this bridge were used. The sinusoidal wave was resonating on this bridge was changed magnification α of the maximum input acceleration on the basis of 100gal in order to evaluate the dynamic response at the damage time of a plastic hinge part. Moreover, this wave was changed up to 0.25 times, 0.50 times, 0.75 times, 1.00 times, 1.25 times, 1.50 times, and a maximum of 5.00 times. Furthermore, the input seismic wave changed the magnification α of the maximum input acceleration up to 0.10 to 1.00 times. This section considered transition of the maximum response ductility factor in a plastic hinge part assumed each bridge pier to the maximum

Table 2 List of Maximum response ductility factor

(a) The sinusoidal wave

α	Max input acc.(gal)	Maximum response ductility factor					
		P1top	P1bottom	P2top	P2bottom	P3top	P3bottom
0.25	25.000	0.141	0.057	0.051	0.057	0.146	0.065
0.50	50.000	0.332	0.195	0.197	0.180	0.322	0.226
0.75	75.000	0.571	0.446	0.460	0.432	0.541	0.484
1.00	100.000	0.817	0.702	0.724	0.687	0.764	0.747
1.25	125.000	1.276	0.969	0.981	0.986	0.988	1.011
1.50	150.000	2.110	1.754	1.781	1.328	1.495	1.604
2.00	200.000	2.963	2.683	2.683	1.917	2.198	2.367
2.50	250.000	3.994	3.720	3.412	2.548	2.644	2.971
3.00	300.000	4.432	4.215	3.797	2.871	3.506	3.766
4.00	400.000	5.389	6.345	5.480	4.416	5.653	5.880
5.00	500.000	7.037	7.818	7.043	5.404	7.123	7.133

(b) TYPE II – I – 1

α	Max input acc.(gal)	Maximum response ductility factor					
		P1top	P1bottom	P2top	P2bottom	P3top	P3bottom
0.10	81.202	0.218	0.076	0.069	0.073	0.167	0.075
0.20	162.404	0.476	0.322	0.321	0.287	0.361	0.271
0.30	243.606	0.759	0.601	0.588	0.559	0.561	0.559
0.40	324.808	1.085	0.891	0.863	0.839	0.767	0.855
0.50	406.010	2.115	1.866	1.619	1.377	0.972	1.540
0.60	487.212	2.890	2.671	2.676	1.961	1.630	2.271
0.70	568.414	3.256	2.989	3.296	2.210	2.638	2.779
0.80	649.616	3.283	3.876	4.598	3.107	3.885	3.915
0.90	730.818	4.746	5.491	5.954	4.073	5.237	5.244
1.00	812.020	6.361	7.180	7.217	5.113	6.606	6.616

(c) TYPE II – II – 1

α	Max input acc.(gal)	Maximum response ductility factor					
		P1top	P1bottom	P2top	P2bottom	P3top	P3bottom
0.10	68.683	0.184	0.065	0.071	0.076	0.195	0.082
0.20	137.366	0.414	0.255	0.338	0.292	0.418	0.338
0.30	206.049	0.665	0.506	0.619	0.563	0.659	0.609
0.40	274.732	0.899	0.769	0.901	0.832	0.896	0.884
0.50	343.416	1.409	1.060	1.508	1.197	1.363	1.514
0.60	412.099	2.564	2.267	2.067	1.658	1.638	1.884
0.70	480.782	4.008	3.588	3.199	2.467	1.864	2.973
0.80	549.465	5.151	4.732	4.288	3.168	2.407	3.892
0.90	618.148	6.119	5.822	5.378	3.855	3.051	4.754
1.00	686.831	7.267	7.048	6.377	4.615	3.944	5.728

(d) TYPE II – III – 1

α	Max input acc.(gal)	Maximum response ductility factor					
		P1top	P1bottom	P2top	P2bottom	P3top	P3bottom
0.10	59.103	0.241	0.104	0.084	0.083	0.194	0.080
0.20	118.207	0.512	0.388	0.367	0.342	0.410	0.336
0.30	177.310	0.793	0.675	0.626	0.614	0.603	0.631
0.40	236.414	1.159	0.966	0.887	0.886	0.818	0.925
0.50	295.517	2.182	2.080	1.584	1.441	0.993	1.718
0.60	354.620	3.046	2.708	2.680	1.898	1.604	2.257
0.70	413.724	3.565	2.965	3.201	2.237	2.456	2.822
0.80	472.827	3.845	3.265	4.459	2.940	3.354	3.702
0.90	531.931	3.979	4.673	5.750	3.652	4.309	4.439
1.00	591.034	4.678	5.594	6.616	4.201	5.092	5.343

input acceleration. Here, it is considered as the value that broke the maximum response rotation angle in a plastic hinge part by the yield rotation angle with the maximum response ductility factor. When the value exceeds 1.0, it means that a plastic hinge part of a bridge pier reaches the yield limit state. The list of the maximum response ductility factor is shown in Table 2, and the relationship between the maximum ductility factor and the maximum input acceleration is shown in Fig.7. From this analysis results, the maximum response ductility factor of each bridge pier was the order of the bottom end of P1 bridge pier, P1 bridge pier top end, the bottom end of P3 bridge pier, P3 bridge pier top end, P2 bridge pier top end, and the bottom end of P2 bridge pier fundamentally, after all bridge piers reached the yield limit state. However, when the plastic hinge of each bridge pier approached the ultimate limit state, the bending damage growth of this analysis model was not necessarily in agreement. Moreover, in Fig.7(a) and (c), the inversion of the maximum response ductility factor of P1 bridge pier and P3 bridge pier had been checked. It was thought that it was based on the influence of unequal bridge pier height as a reason that the maximum response ductility factor reversed. Furthermore, in Fig.7(c) and (d), it had checked that bending damage was progressing to the input seismic wave with long period component relatively. The same tendency as the sinusoidal wave was resonating on this bridge in Fig.7(a) was seen. Therefore, it is necessary to evaluate with accuracy sufficient about the influence of the frequency characteristic of the input earthquake motion, about the bending damage growth in this dynamic response analysis results.

4. Damage index

Before arguing about energy absorption, not only the maximum deformation but the energy absorption of each plastic hinge part was united and considered about damage evaluation of the continuation rigid frame bridge. Park's damage index³⁾ was the standard of the damage expressed with the sum of the

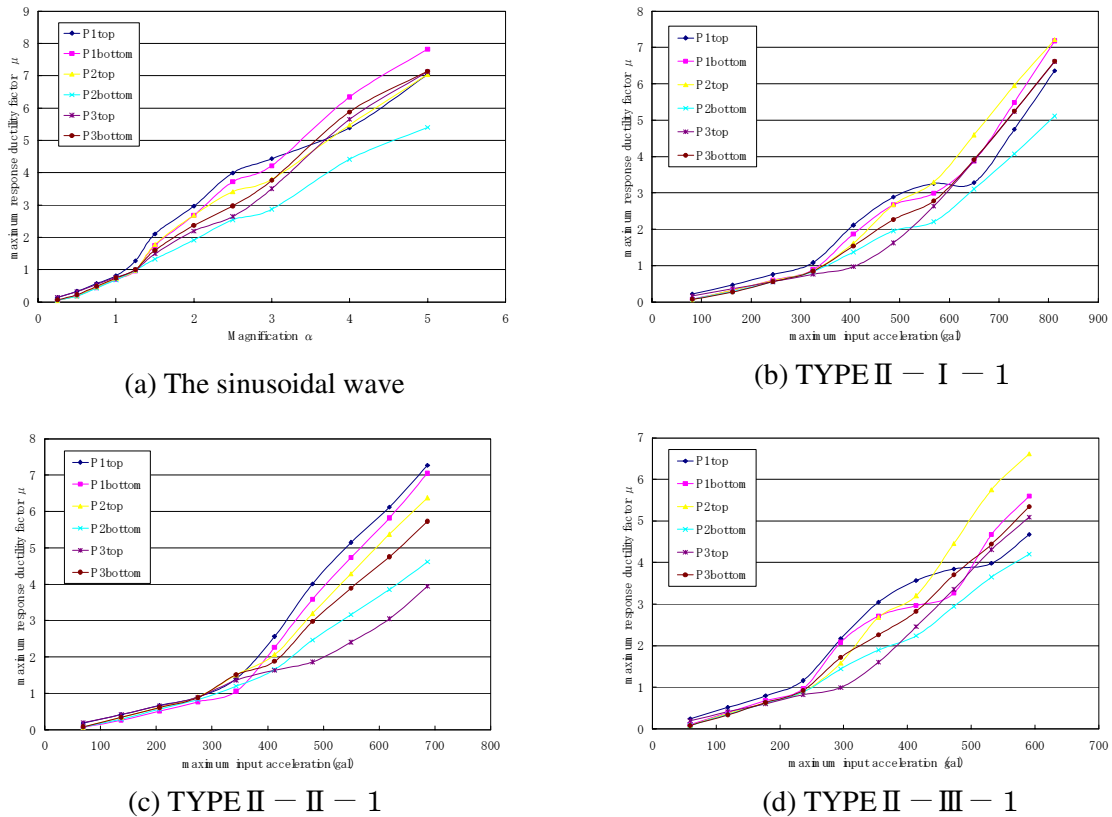


Fig.7 Relationship between Maximum input acceleration and Maximum response ductility factor

maximum deformation and increment of the consumption energy to the damage grade about a reinforced concrete member cyclic-loaded. Park's damage index D was shown in the following formula.

$$D = \frac{\delta_M}{\delta_u} + \frac{\beta}{Q_y \delta_u} \int d E$$

$$\beta = (- 0.447 + 0.073 \frac{l}{d} + 0.24 n_o + 0.134 p_t) \cdot 0.7 p_w$$

- Here, δ_M ; Maximum deformation sustained by member
 δ_u ; Ultimate deformation under static loading
 Q_y ; Yield horizontal strength of a reinforced concrete pier
 $d E$; Incremental absorbed hysteretic energy
 l / d ; Effective span ratio
 n_o ; Normalized axial stress
 p_t ; Tension steel ratio
 p_w ; Confinement ratio

Moreover, the maximum deformation of the structure used the response displacement about Park's damage index. However, in this examination, it arranged using the response rotation angle prepared in each plastic hinge part. Furthermore, Q_y was the yield horizontal strength of a reinforced concrete pier, but the yield bending moment was used considering the relation of $M - \theta$. Therefore, it asked for the damage index D by the formula shown below. In this study, the value of β used 1.0.

$$D = \frac{\theta_M}{\theta_u} + \frac{\beta}{M_y \theta_u} \int d E$$

- Here, θ_M ; Maximum response rotation angle of a reinforced concrete pier
 θ_u ; Ultimate response rotation angle of a reinforced concrete pier
 M_y ; Yield bending moment of a reinforced concrete pier
 $d E$; Incremental absorbed hysteretic energy

Table 3 List of Damage index

(a) The sinusoidal wave

α	Damage index D					
	P1top	P1bottom	P2top	P2bottom	P3top	P3bottom
0.50	0.013	0.009	0.009	0.009	0.013	0.010
0.75	0.022	0.023	0.023	0.025	0.023	0.025
1.00	0.032	0.039	0.037	0.041	0.034	0.041
1.25	0.049	0.054	0.051	0.059	0.044	0.058
1.50	0.082	0.108	0.113	0.088	0.072	0.107
2.00	0.115	0.205	0.199	0.152	0.118	0.189
2.50	0.154	0.309	0.271	0.219	0.159	0.260
3.00	0.171	0.393	0.319	0.275	0.238	0.349
4.00	0.208	0.619	0.505	0.424	0.470	0.549
5.00	0.272	0.891	0.692	0.610	0.621	0.791

(b) TYPE II – I – 1

α	Damage index D					
	P1top	P1bottom	P2top	P2bottom	P3top	P3bottom
0.40	0.042	0.047	0.041	0.048	0.034	0.046
0.50	0.082	0.133	0.100	0.090	0.044	0.100
0.60	0.118	0.213	0.224	0.161	0.146	0.199
0.70	0.126	0.291	0.315	0.226	0.179	0.265
0.80	0.127	0.391	0.406	0.309	0.285	0.378
0.90	0.184	0.554	0.536	0.408	0.390	0.513
1.00	0.246	0.700	0.625	0.495	0.502	0.628

(c) TYPE II – II – 1

α	Damage index D					
	P1top	P1bottom	P2top	P2bottom	P3top	P3bottom
0.30	0.025	0.028	0.031	0.033	0.028	0.033
0.40	0.035	0.044	0.046	0.050	0.041	0.049
0.50	0.054	0.060	0.090	0.074	0.070	0.097
0.60	0.099	0.182	0.179	0.139	0.094	0.172
0.70	0.155	0.308	0.274	0.219	0.142	0.279
0.80	0.199	0.426	0.360	0.293	0.195	0.363
0.90	0.237	0.523	0.443	0.356	0.247	0.440
1.00	0.281	0.625	0.513	0.420	0.315	0.522

(d) TYPE II – III – 1

α	Damage index D					
	P1top	P1bottom	P2top	P2bottom	P3top	P3bottom
0.30	0.031	0.035	0.031	0.036	0.027	0.035
0.40	0.045	0.053	0.045	0.053	0.038	0.052
0.50	0.084	0.146	0.102	0.097	0.047	0.118
0.60	0.118	0.228	0.234	0.166	0.091	0.210
0.70	0.138	0.307	0.327	0.239	0.166	0.290
0.80	0.149	0.407	0.446	0.319	0.255	0.390
0.90	0.154	0.514	0.563	0.397	0.344	0.485
1.00	0.181	0.616	0.650	0.458	0.419	0.566

5. Energy absorption characteristic

At present, Park's damage index in consideration of the maximum deformation and the increment of consumption energy was used as the evaluation method of energy absorption characteristic. The calculation result of the damage index is shown in Table 3. In Fig.8, the grade of damage changed with maximum input acceleration in the plastic hinge part of each bridge pier. Moreover, the relationship between the magnification α of the maximum input acceleration and the damage index D is shown in Fig.8. From this analysis results, the damage index of each bridge pier became small in order of the bottom end of P1 bridge pier, the bottom end of P3 bridge pier, P2 bridge pier top end, P3 bridge pier top end, the bottom end of P2 bridge pier, and P1 bridge pier top end fundamentally. However, the bottom end of P2 bridge pier and P3 bridge pier top end were reversed by only Fig.8(c). Next, the bottom end of P2 bridge pier and the bottom end of P3 bridge pier were reversed by only Fig.8(d). Furthermore, as shown in Fig.8(d), the inversion of the bridge pier that showed the maximum damage index had been checked. Subsequently, in the plastic hinge part of each bridge pier, it became a different thing from the tendency that the damage index showed as compared with the tendency of the maximum response ductility factor. Therefore, the correlation nature about the maximum response ductility factor and the damage index in the plastic hinge part was not necessarily accepted. Moreover, in Park's damage index, even if it compared with the bending damage growth of pushover analysis, it was not necessarily in agreement.

CONCLUSION

By this study, the failure type of the whole bridge system set up the analysis model the bending failure will occur first. Here, the ultimate horizontal strength of the bridge pier was the same, and it was aimed

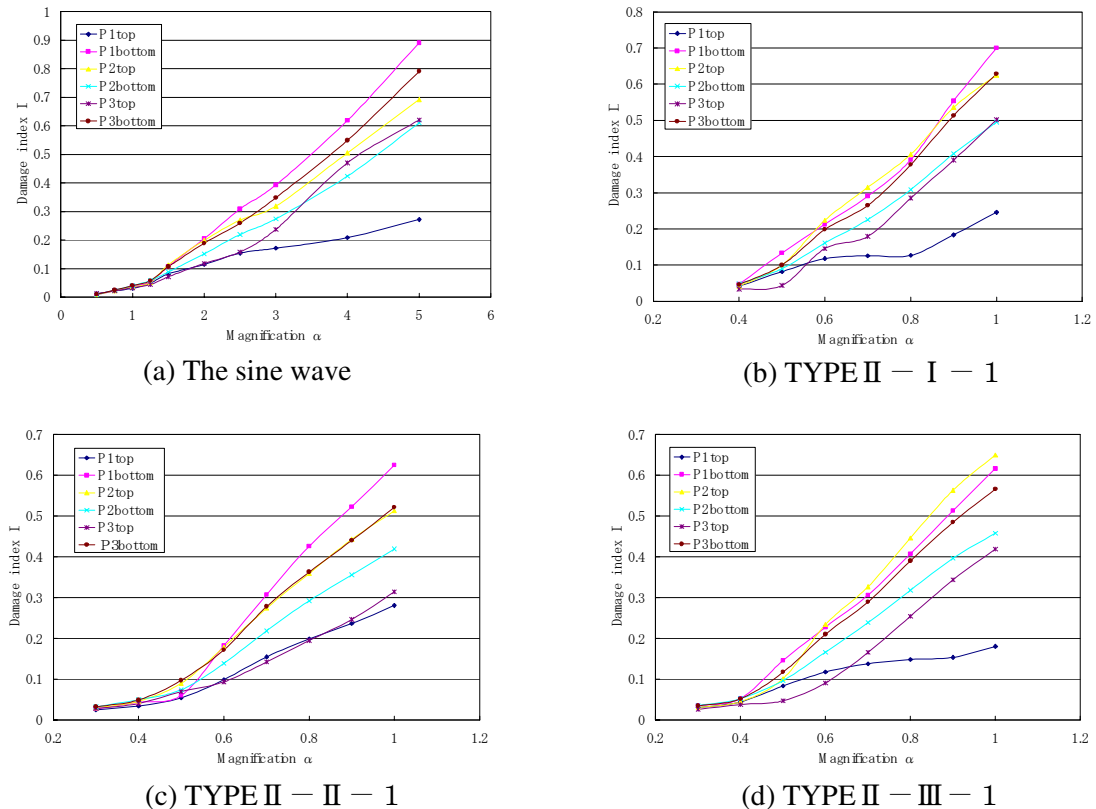


Fig.8 Relationship between Magnification and Damage index

at the longitudinal direction to the bridge axis of the continuation rigid frame bridge with unequal piers. Moreover, pushover analysis and dynamic response analysis were carried out for the longitudinal direction to the bridge axis, and some considerations were added about bending damage growth. Furthermore, its attention was paid to the energy absorption in each plastic hinge part of the continuation rigid frame bridge.

The acquired knowledge is enumerated below.

(1) From this pushover analysis results, the order of bending damage growth differed by the input time of the direction of $P1 \rightarrow P3$ and the input time of the direction of $P1 \leftarrow P3$. The reason the order of damage progress differed was considered that the change of bridge pier height had influenced.

(2) From this dynamic response analysis results, it has checked that bending damage was progressing to the input seismic wave with long period component relatively. Moreover, the same tendency was seen as the sinusoidal wave on this bridge.

(3) It was not necessarily in agreement, as a result of comparing about Park's damage index and the maximum response ductility factor after each plastic hinge part surrendered.

In this study, it was analyzing only about the continuation rigid frame bridge that has one kind of unequal bridge pier height. Then, Park's damage index in consideration of both maximum deformation and energy absorption was used. Therefore, it is thought that it is effective as the technique of evaluating damage rationally to take two parameters into consideration appropriately. However, it is necessary to evaluate with accuracy sufficient about the influence of the frequency characteristic of the input earthquake motion in dynamic response analysis. Moreover, I think it an important future subject to define the ultimate limit state of the whole bridge system. Furthermore, it is required to examine the evaluation technique of bending damage growth and energy absorption characteristic in details more.

REFERENCES

1) Japan Road Association : Specifications for Highway Bridges Part V ; Seismic Design, Maruzen, Tokyo, March 2002.

2) Hamamoto, Mazda, Otsuka, and Tsukuda : Analytical study on damage of a continuous rigid frame bridge with unequal piers, Proceedings of the Japan Concrete Institute, Vol.25, No.2, pp.1393-1398, July 2003.

3) Rark, Y.-J, and Ang, A.H.-S : Mechanistic seismic damage model for reinforced concrete, Journal of Structural Engineering, Vol.111, No.4, pp.722-739, April 1985.